

---

## An agent- based model accurately predicts larval dispersal and identifies restoration and monitoring priorities for eastern oyster ( *Crassostrea virginica* ) in a Southwest Florida estuary

Dye Bass <sup>1,2,\*</sup> , Jose Felix <sup>1</sup> , Richard Joëlle <sup>1,3</sup> , Mortensen Jonas Brandt <sup>4</sup> , Milbrandt Eric C. <sup>5</sup>

<sup>1</sup> Department of Marine and Earth Sciences Florida Gulf Coast University Fort Myers FL 33965 ,U.S.A.

<sup>2</sup> Department of Coastal Systems NIOZ Royal Netherlands Institute for Sea Research P.O. Box 59, 1790 Alberta, Den Burg Texel, The Netherlands

<sup>3</sup> University of Brest, Ifremer CNRS, UMR 6308, AMURE, Unité d'Economie Maritime, IUEM Plouzané 29280 ,France

<sup>4</sup> DHI A/S., Agern Allé 5, DK-2970 Hørsholm, Denmark

<sup>5</sup> Marine Laboratory Sanibel-Captiva Conservation Foundation 900A Tarpon Bay Road Sanibel, FL 33957 ,U.S.A.

\* Corresponding author : Bass Dye, email address : [bass.d.dye@gmail.com](mailto:bass.d.dye@gmail.com)

---

### Abstract :

An agent-based modeling (ABM) framework was developed to support oyster reef restoration efforts in the Caloosahatchee River Estuary located within the encompassing Charlotte Harbor estuarine system, Southwest Florida. The modeling approach is novel for this shallow estuary which experiences heavily managed freshwater inflow known to be an ecological stressor to the estuary's oysters. The aims of the study were to (1) determine the ABM's accuracy in simulating larval dispersal patterns when compared with measured in situ larval settlement data; (2) establish connectivity patterns between various oyster reefs within the estuary; and (3) discover larval transport pathways within the Charlotte Harbor estuarine system. Key characteristics of the ABM, in particular the agents serving as simulated larvae, include settlement behavior and salinity tolerance and associated mortality. The ABM accurately recreated larval dispersal patterns during the peak spawning season, providing fundamental insight into the importance of protecting the furthest upstream oyster reef as a sustained larval source to the downstream reefs. Thus, supporting the effectiveness of using field measurements for the validation of ABMs and subsequently using ABM simulations to bolster future field studies. Ultimately, this study provides an effective, generally applicable, approach to model larval ecology for restoration purposes.

**Keywords** : ABM Lab, agent-based model, Caloosahatchee River Estuary, larval transport and dispersal, MIKE ECO Lab template, population connectivity

54

55

## **Implications for Practice**

56

57

- A novel approach to study oyster larval transport and dispersal within the Caloosahatchee

58

River Estuary and the broader Charlotte Harbor estuarine system was performed using an

59

agent-based model (ABM).

60

- The ABM incorporates agent (oyster larvae) settlement behavior and salinity related

61

tolerances and mortality which, when validated with existing field data, provides insight

62

into an upstream oyster reef as a vital larval source.

- 63       • This study was able to develop a working, generally applicable modelling framework  
64       serving as the foundation for future modeling and field based studies focused on oyster  
65       reef restoration.

66  
67 **Introduction**

68  
69       Oyster reefs have declined in many estuarine and coastal ecosystems from overharvesting,  
70       diseases, and deteriorated water quality (Beck et al. 2011). The once flourishing Chesapeake Bay  
71       oyster population has been reduced to 1 percent of its historical abundance from a myriad of issues  
72       (Rothschild et al. 1994). In 2012, Florida’s Apalachicola Bay, a region producing 10 percent of  
73       the United States’ annual oyster harvest, experienced an oyster fishery collapse attributed to low  
74       juvenile survival in the years prior to the collapse (Pine et al. 2015). Although the Caloosahatchee  
75       River Estuary (hereinafter CRE) does not support a commercial oyster fishery, the estuary’s oyster  
76       reefs are valued ecosystem components (Chamberlain & Doering 1998; Barnes et al. 2007).

77       Historically, the CRE (Fig. 1 cross hatch region) located in Southwest Florida supported  
78       extensive *Crassostrea virginica* (Eastern oyster) reefs; however oyster reef removal and man-made  
79       alterations to the estuary’s hydrology have reduced the oyster population (Chamberlain & Doering  
80       1998). Presently, CRE oysters experience vastly differing freshwater inflow depending on the  
81       season as Florida’s subtropical climate produces wet (June-Oct.) and dry (Nov.-May) seasonal  
82       patterns. In addition, a lock and dam structure (S-79) controls 70% of the freshwater entering the  
83       estuary (Sun et al. 2016). Typically, freshwater releases from the dam are minimal during the dry  
84       season. In contrast, the estuary can be driven fresh by high inflow throughout the wet season  
85       (Chamberlain & Doering 1998) coinciding with the oyster’s spawning period (late spring to early  
86       fall; Volety et al. 2015). Therefore, large pulsed and or sustained inflow may result in larval

87 mortality, downstream larval flushing, and or larvae flushed entirely out of the estuary  
88 (Chamberlain & Doering 1998; Volety et al. 2015).

89         Prior studies have been conducted within the estuary regarding inflow, oyster health, and  
90 habitat. Altered hydrology, including the unnaturally high and low inflow, has been identified as  
91 the key ecological stressor within the CRE (Barnes 2005). Barnes (2005) identified additional key  
92 CRE stressors (estuarine salinity, inflow, nutrient inputs, and physical alterations) which were  
93 implemented into a CRE habitat suitability index model (HSI). The HSI study by Barnes et al.  
94 (2007) found preferred inflow conditions (i.e. seasonally managed frequency distribution of  
95 inflow) and storing excess inflow in a constructed reservoir would provide more suitable habitat  
96 conditions than existing conditions without management. Volety et al. (2009) labelled the CRE  
97 oyster population at stage “caution” by accounting for biological responses (e.g. oyster density,  
98 larval recruitment, disease prevalence) and the estuary’s hydrological conditions (temperature and  
99 salinity). Buzzelli et al. (2013) simulated potential oyster densities resulting from varying inflow  
100 thereby providing a range of inflow to promote healthy oyster densities. However, agent-based  
101 modeling of oyster larval transport (larval movement between two locations), considering the  
102 behavioral aspects of the agents (larvae), and dispersal (spread of larvae from spawning source to  
103 settlement site; Pineda et al. 2007) has not been conducted for the CRE and was recommended by  
104 Volety et al. (2015) as an important future study to better understand the influence of inflow on  
105 CRE oyster populations.

106         Previous studies by Kim et al. (2010, 2013) in Mobile Bay, Alabama utilized a  
107 hydrodynamic and larval transport model along with field data to investigate Eastern oyster larval  
108 transport and dispersal patterns under both realistic and idealized physical transport scenarios.  
109 Those studies provided a better understanding of larval movement among Mobile Bay’s various

110 regions and associated oyster reefs, thus providing a management tool to aid in the development  
111 and implementation of oyster reef restoration strategies. The ability to predict larval transport and  
112 dispersal under different inflow conditions is critical to a highly managed system because  
113 interannual differences in inflow could shift the target for oyster reef restoration from upstream  
114 (dry years) to downstream (wet years). A system-wide approach should consider adult oyster  
115 suitability indicators such as salinity, reef elevation, food supply, and substrate availability (Barnes  
116 et al. 2007). Additional consideration is needed to determine reef connectivity and larval supply  
117 for restoring and maintaining estuarine oyster populations. The present study uses an agent-based  
118 model (ABM) comprised of a hydrodynamic model of the Charlotte Harbor estuarine system (Dye  
119 et al. 2020) and an ecological modeling module (MIKE ECO Lab; DHI 2017) to simulate oyster  
120 larval transport and dispersal within the CRE and the larger, encompassing Charlotte Harbor  
121 estuarine system hereafter CHES (Fig. 1). MIKE ECO Lab is a process-based customizable  
122 ecosystem modeling tool widely used to study the transport, dispersal, as well as foraging traits of  
123 various organisms such as eelgrass, coral larvae, starfish, sea birds, and marine mammals (Tay et  
124 al. 2012; Elsäßer et al. 2013; Canal-Vergés et al. 2014; Heinänen et al. 2018; Kussemäe et al. 2018;  
125 Cavalcante et al. 2020). The MIKE ECO Lab model template created specifically for *C. virginica*  
126 oyster larvae was tested in its ability to simulate dispersal patterns observed in situ the CRE.  
127 Furthermore, simulated model outputs were used to: (1) establish the connectivity patterns between  
128 the monitored oyster reef sites and (2) determine larval transport within the CHES.

## 129 **Materials and Methods**

### 130 **Site Description**

131 The CHES is a large (~700-800 km<sup>2</sup>), shallow, subtropical estuary located in Southwest  
132 Florida with an average microtidal range of 0.6 m (Scarlatos 1998). Marine water from the Gulf

133 of Mexico enters the estuary through various inlets (e.g., Gasparilla Pass, Boca Grande Pass,  
134 Captiva Pass, Redfish Pass, Blind Pass, San Carlos Bay; Fig. 1) between the barrier islands as well  
135 as San Carlos Bay. Freshwater enters the CHES by precipitation, watershed runoff, and three  
136 rivers; Myakka and Peace Rivers supply the northern portion while the Caloosahatchee River  
137 supplies freshwater to the southern region.

138 Located in the southern region of the CHES, the CRE (Fig. 1 cross hatch region) has depths  
139 ranging from 0.3–6.0 m (1.5 m mean depth; Scarlatos 1988). Various man-made changes have  
140 altered the morphology and hydrology of the CRE. In the late 1800s the Caloosahatchee River was  
141 artificially connected to Lake Okeechobee (Flaig et al. 1998). Modifications continued as the  
142 Caloosahatchee River, originally a meandering river, was straighten and deepened, and three lock  
143 and dam structures were constructed to improve flood control measures of Lake Okeechobee (Sun  
144 et al. 2016). Additionally, the furthest downstream lock and dam (S-79) acts as a salinity barrier  
145 between the fresh river water and the estuary's brackish water (Chamberlain & Doering 1998; Sun  
146 et al. 2016). The CHES is unique because of the more natural conditions in the northern region as  
147 compared to the very unnatural, man-made conditions in the CRE portion of the system.

## 148 **The Model**

149 This ABM presented in this study was built in ABM Lab, the Lagrangian module available  
150 in MIKE ECO Lab (DHI 2017), in order to describe Eastern oyster, *C. virginica*, larval transport  
151 within the CHES and more specifically larval transport and dispersal within the CRE (Fig. 1 cross  
152 hatch region). The Eulerian-Lagrangian modelling framework applied in this study consists of a  
153 MIKE 21 hydrodynamic flexible mesh model (HD) (DHI 2016) integrated with the MIKE ECO  
154 Lab (DHI 2017) ecological modeling module. The HD uses a finite volume method to solve  
155 shallow water, depth-integrated incompressible Reynolds averaged Navier-Stokes Equations (DHI

156 2016). The MIKE ECO Lab module provides a customizable model template for users to develop  
157 mathematical equations and descriptions of target species, including their behavioral tendencies,  
158 and the environmental parameters (e.g. state variables, constants, forcing). The physical  
159 environment was simulated by the HD and the Eastern oyster-specific mathematical equations and  
160 descriptions were customized in the MIKE ECO Lab template for the study area. The movement  
161 and environmental interaction of simulated oyster larvae, hereinafter referred to as agents, were  
162 modelled by the overarching ABM.

163 The model description follows the ODD (Overview, Design concepts, Details) protocol  
164 (Grimm et al. 2006, 2010) for describing individual and agent-based models developed “to  
165 standardize published model descriptions in order to make descriptions more understandable and  
166 complete.”

### 167 *Purpose*

168 This ABM was developed to test the model’s ability to numerically simulate measured  
169 Eastern oyster larval settlement at four monitored oyster reef sites within the CRE.

### 170 *Entities, State Variables, and Scales*

171 Four groups of agents are simulated with each group representing one of the four oyster  
172 reef locations (Fig. 1, 1-4; Please see **Field Data - In situ oyster and larval characteristics** for  
173 description of reefs). Individuals of each group are characterized by their release site (1-4), position  
174 (x, y, z coordinates), and settlement status (i.e. settled or not settled onto Sites 1-4).

175 An existing HD model of the CHES (Dye et al. 2020) generated the physical environment  
176 (time series of two-dimensional current vectors, surface water elevations, fluxes) for the ABM  
177 under the forcing of realistic wind, tide, and inflow. The HD spatial domain encompasses the entire  
178 CHES, all major tributaries, and extends 80 km offshore into the Gulf of Mexico (Fig. 2 A). The

179 HD accurately simulates the system's water levels, tidal heights, and flow dynamics and has been  
180 used to study the circulation dynamics as well as the effect of inflow and wind on neutrally buoyant  
181 simulated particles within the system (Dye et al. 2020). The HD's flexible triangular mesh (FM)  
182 (DHI 2016) resolution is ~250 m within the focus area of the study (CRE), ~700 m in the  
183 surrounding estuarine regions, and increases to 2.7 km at the outer boundary (Fig. 2A & 2B). A  
184 more detailed model description is provided in Dye et al. 2020.

185 Salinity was included in the ABM by interpolating in situ salinity data from 6 stations  
186 which are part of the RECON monitoring system (<http://recon.sccf.org/>) (Fig. 1, A - G) and 3  
187 gauges deployed and maintained by the Charlotte Harbor Aquatic Preserve in Matlacha Pass (Fig.  
188 1, H - J). Long-term salinity data were collected at each environmental monitoring site within the  
189 study area (Table S1; Fig. 1, A - J) and interpolated (distance weighted) into a high-resolution grid  
190 for the model domain, grid resolution of ~200m (Fig. 2C). Hourly salinity values were extracted  
191 using the DHI MATLAB Toolbox ([https://github.com/DHI/DHI-MATLAB-](https://github.com/DHI/DHI-MATLAB-Toolbox/blob/master/Documentation/DHI_MATLAB_Toolbox_User_Guide.pdf)  
192 [Toolbox/blob/master/Documentation/DHI\\_MATLAB\\_Toolbox\\_User\\_Guide.pdf](https://github.com/DHI/DHI-MATLAB-Toolbox/blob/master/Documentation/DHI_MATLAB_Toolbox_User_Guide.pdf)). The resulting  
193 two-dimensional grids were converted into dfs2 file format and subsequently converted into a  
194 MIKE ECO Lab compatible file.

### 195 ***Process Overview and Scheduling***

196 The simulation was executed with an 8 second time step in the following order:  
197 hydrodynamics, advection-dispersion, salinity, agent sensitivity to salinity (discussed in section  
198 Sensing), agent movement (x,y,z), and agent settlement behavior (discussed in section Basic  
199 Principles).

### 200 ***Design Concepts***

#### 201 ***Basic Principles***



202 Agents were released in the model domain from the sites (Fig. 1, 1-4) found to be spawning  
203 during the study period (please see sections Field data and Simulation for further description).  
204 Every agent is considered a successfully fertilized zygote and therefore capable of development  
205 into a competent larva. During the simulation, every agent becomes competent (i.e. larvae has  
206 metamorphosed into the pediveliger stage thereby developing a foot to search for and subsequently  
207 attach (settle) onto hard substrate (Wallace et al. 2008)) to settle if the agent survives beyond the  
208 development period (Table 1).

209 Four requirements must be fulfilled for an agent to successfully settle onto a mesh grid cell  
210 classified as a settlement substrate (Fig. 1, 1-4). (1) An agent has developed and gained  
211 competency, (2) an agent's x, y coordinates in a given model time step coincide with a settlement  
212 substrate, (3) the agent is less than 0.5 m away from the settlement substrate, and (4) the current  
213 velocity must be less than 1.0 m/s at the time step of settlement (Table 1). Once agents settle onto  
214 a settlement substrate, the agents are considered successfully settled and are no longer subjected  
215 to any mortality, natural or salinity-based (please see sections Sensing and Stochasticity for further  
216 details).

217 Agent transport is regulated by current direction and velocities – both horizontal and depth-  
218 averaged vertical velocities – as well as settling velocities assigned to agents (Table 1). During  
219 the development period an agent is assigned a neutral buoyancy with a settling speed of 0 m/s.  
220 Once an agent has progressed through the development period and is thereby competent to settle,  
221 an agent is assigned a settling speed of 0.007 m/s (Table 1).

222 *Adaptation*

223           After gaining competency, an agent will actively swim towards the benthic zone in a  
224 settlement attempt if the agent, in its current simulation time step, is located within a model mesh  
225 cell designated as settlement substrate (Fig. 1, 1-4).

#### 226 *Sensing*

227           Specific salinity tolerance ranges for agents and the complementing time durations were  
228 included in the MIKE ECO Lab template (Table 2). Agent salinity tolerance ranges (Davis 1958;  
229 Davis & Calabrese 1964) provide the lower threshold of salinity values before salinity timers are  
230 initiated. The required durations that agents must spend above each salinity threshold to reset the  
231 duration timer were user-defined, however durations were largely based on the study by Kinne &  
232 Kinne (1962). If the salinity duration timer for an individual agent exceeds the maximum time in  
233 the corresponding salinity range (Table 2), the agent is classified as dead and removed from the  
234 simulation.

#### 235 *Stochasticity*

236           A constant horizontal dispersion value, based on hydrodynamic model resolution, was  
237 assigned throughout the model domain (Table 1) because of the importance of horizontal  
238 dispersion (i.e. transport from non-resolved turbulence or eddies in numerical models) in coastal  
239 and estuarine environments (Geyer & Signell 1992). No vertical dispersion was included in the  
240 template. Considering the shallow nature of the study area, it is safe to assume that horizontal  
241 dispersion is the primary mode of agent transport (Suara et al. 2018). Additionally, particle  
242 resuspension was activated in the ABM which forces agents contacting the benthic substrate back  
243 into resuspension unless the agents have settled onto a suitable substrate.

244           To reduce the overestimation of agent survival (Connolly & Baird 2010; Tay et al. 2012),  
245 natural mortality, beginning at the time of agent release, was included by an age-dependent

246 decreasing Weibull function mimicking a Type III survivorship curve (Pinder et al. 1978; Table  
247 1).

### 248 *Collectives*

249 One individual collective of agents is assigned to each of the four sites. No differences  
250 exist between the collectives apart from their release location from one of the four sites. All state  
251 variables and traits are consistent for all agents within the simulation, regardless of collective.

### 252 *Observations*

253 Outputs obtained from the model include agent location (x, y), total surviving (i.e. non  
254 settled agents remaining in simulation) agents, and agent settlement assessed at each site (1-4).  
255 Outputs were saved every 1 hour, however only outputs at the final time step (conclusion of  
256 simulation) were used to determine transport patterns and for further comparison with field data  
257 collected from the study area.

### 258 *Initialization*

259 Twenty-five hundred agents were released from the individual sites during the 25 day  
260 simulations, thus representing a typical larval duration (Kennedy 1996; Narvaez et al. 2012).  
261 Natural variability as well as uncertainty exists in the literature regarding the specific values chosen  
262 to represent the larval characteristics (e.g. larval salinity tolerance ranges) (Tay et al. 2012).  
263 Therefore, all values (Tables 1 and 2) were kept constant throughout each simulation to normalize  
264 comparisons between the different simulations.

### 265 *Input data*

266 Forcing of this ABM model were obtained from the HD (water levels, current velocities  
267 and direction; Dye et al. 2020) and the two-dimensional depth-averaged salinity grids (Table 1).

### 268 **Sensitivity Analysis**

269           Since it was unknown how many larvae were released at each site during the spawning  
270 periods, model sensitivity to the number of agents released was tested. The sensitivity analysis  
271 provided an understanding of any difference between larval recruitment success and number of  
272 larvae (agents) released. Sensitivity analysis was performed for August 2011 by releasing 2,500,  
273 5,000, or 10,000 agents from Sites 1 and 3 in three separate simulations. The relative percentage  
274 of agent settlement at the Sites 1-4 were compared to determine any relative variability between  
275 simulations. Differences in percent total settlement at the four sites consisted of 1.04% between  
276 simulations releasing 2,500 and 5,000 and 0.38% between simulations releasing 5,000 and 10,000  
277 agents (Table 3). This decreasing trend in the percentage of settlement with greater amounts of  
278 agents released occurred at Sites 2 and 3 with less than 0.46% differences in percent settlement  
279 between simulations (Table 3). At Sites 1 and 4, settlement percentage was lowest during the 5,000  
280 agent release simulations. Minor differences in percent settlement of 0.02% occurred between  
281 simulations at Site 4 while greater differences of 0.16% resulted between simulations at Site 1  
282 (Table 3). Sensitivity analysis provided evidence that greater amounts of agents released did not  
283 drastically enhance settlement and differences can be partially attributed to randomness in the  
284 stochastic processes of both dispersion and particle process descriptions. Therefore, it was decided  
285 to release 2,500 agents at the respective sites in each simulation.

### 286 **Field Data - In situ oyster and larval characteristics**

287           A long-term (2000-2016), oyster monitoring study was performed by Volety et al. (2015)  
288 at four oyster reef sites (Fig. 1, 1-4) along the CRE's salinity gradient. Site 1 marks the farthest  
289 upstream extent of living oysters, and Sites 2 – 4 are situated progressively downstream within  
290 increasingly higher salinity regimes. Live oyster density is generally high, exceeding 800  
291 oysters/m<sup>2</sup> at all sites except at Site 1 during years of extremely high inflow. Adult oysters are

292 reproductively active in the summer months (May - October) with larval settlement subsequently  
293 peaking (June - November) and correlated with inflow (i.e. reduced settlement with high inflow;  
294 Volety et al. 2015). The 2011 field season provided larval settlement and histological analysis data  
295 used in this study.

296 Larval settlement was evaluated monthly from the four sites by deploying three shell  
297 strings suspended within the water column, approximately 10-15 cm above the bottom of the  
298 estuary. Each shell string consisted of 12 oyster shells with a shell heights of about 5.0-7.5 cm,  
299 stacked inner shell surface oriented downwards, and suspended by galvanized wire via PVC poles  
300 (Volety et al. 2015). Field measurements of larval settlement were compared with simulated  
301 settlement to test the model's ability to accurately reproduce the measured settlement patterns.

302 Histological analysis was performed to determine the reproductive state of oysters within  
303 the estuary using methods by Fisher et al. (1996) and the International Mussel Watch Program  
304 (1980). Each month, ten oysters were collected, analyzed, and assigned a value ranging from 1-5  
305 indicating the oyster's gonadal condition. Gonad index values ranging from 4-5 were classified as  
306 oyster spawning events and subsequently used to determine from which site to release agents  
307 within the model simulations.

### 308 **ABM Simulations**

309 Individual model simulations were performed for the months of July, August, and  
310 September 2011 with monthly simulation periods coinciding with observed site specific spawning  
311 (Table 4). Agents were released synchronously on the 5<sup>th</sup> of each simulation month, one hour after  
312 the larger high tide, during the ebbing tide. Uncertainty in the timing of oyster spawning resulted  
313 in the decision to release agents on the ebbing tidal phase as it would provide the "worst case  
314 scenario" for larval retention within the estuarine system.

315 Field measurements determining site specific spawning by means of histological analysis  
316 were conducted within the first week of each month. The model release date (5<sup>th</sup> of each month)  
317 was chosen to standardize the simulations and reduce field measurement bias as much as possible.  
318 Twenty-five hundred agents were released from the individual sites (Table 4; Fig. 1, 1-3) indicated  
319 by the field observations to be spawning based on the gonad index values. The simulations were  
320 conducted for 25 days to represent a typical planktonic larval phase (Kennedy 1996; Narvaez et  
321 al. 2012).

## 322 **Comparison of Simulated and Observed Larval Settlement within the CRE**

323 In situ oyster settlement measurements (see **Field Observations - In situ oyster and larval**  
324 **characteristics**) were compared to the simulated settlement to test model performance in  
325 predicting observed settlement. However, simulated settlement does not account for post-larval  
326 settlement mortality (Osman et al. 1989; Narvaez et al. 2012) and cannot be directly compared to  
327 the observed measurements in terms of magnitude. Therefore, comparisons between simulated and  
328 observed settlement are in terms of trends, an ecologically viable method used by Narvaez et al.  
329 (2012), with differences indicating the potential importance of post-settlement mortality.

330 Variability existed between element sizes of the hydrodynamic model's triangular mesh  
331 which serve as the available settlement substrate at the sites (1-4). Therefore, to normalize the  
332 simulated settlement data, the total simulated larval settlement at each site were divided by the  
333 site's settlement area (m<sup>2</sup> grid size) to calculate a settlement/m<sup>2</sup> value (e.g. settlement density).

## 334 **Results**

### 335 **Percentage of Agent Survival and Settlement**

336 The percentage of agent survival at the end of each simulation period was calculated  
337 ((settled + non settled agents/total # of agents released) x100). Agent survival ranged from 13-

338 16% with lowest survival during the July simulation and highest survival subsequently in August  
339 (Table 5).

340 The percentage of agent settlement for each simulation was additionally calculated ((total  
341 settled/total # of agents released) x100; Table 5). Variability in percentage of settlement existed  
342 between the simulated months. The July simulation experienced the lowest settlement success with  
343 1.2% of released agents successfully settling. Agents experienced the greatest settlement of 3.6%  
344 during August, while the September simulation had a settlement of 2.0%.

### 345 **Comparison of Simulated and Measured Settlement**

346 Figure 3 displays settlement percentage comparisons between the measured (min = 3.3%,  
347 max = 47.0%) and simulated (min = 4.3%, max = 56.3%) settlement at each site for the individual  
348 monthly simulations. The pattern of increased measured settlement from Site 1 to 3 followed by a  
349 reduction at Site 4 is reflected in the simulated data. In July, measured and simulated percentages  
350 at Sites 1 and 2 differed by less than 6.3%, while greater differences (18.3%) were found at Sites  
351 3 and 4. August and September display similar trends between measured and simulated settlement  
352 as July; however, with closer matches at Sites 1 and 3 as compared to Sites 1 and 2 in July (Fig.  
353 3). Generally, the overall simulated settlement was greater than the measured settlement at Sites  
354 1-3; however, measured settlement was always greater at Site 4.

355 In order to test how well the ABM performs overall in simulating specific site settlement,  
356 comparisons between the percentage ((total settlement from each simulation at a specific site/total  
357 settlement from each simulation at all sites) x100; e.g. (July + Aug. + Sept. settlement at Site 1)/  
358 (July + Aug. + Sept. settlement at all sites) x100) of total measured and simulated settlement at  
359 each individual site are presented in Figure 4. At Site 1, both measured and simulated total  
360 settlement exhibit similar percentages. The measured and simulated settlement at Sites 2 and 3 are

361 within 11.2% of each other, with a lesser proportion of measured settlement at both sites. Although  
362 the simulated settlement is underestimated compared to the measured at Site 4, a trend of  
363 increasing settlement from Site 1 to 3, followed by a reduction in settlement from Site 3 to 4 is  
364 found in both measured and simulated settlement. The ability of the simulations to acceptably  
365 reproduce measured settlement allowed connectivity patterns between the sites to be examined.

### 366 **Connectivity Patterns**

367 Agents were released from Sites 1 and 3 in the July 2011 simulation (Table 4). Self-  
368 recruitment dominated at Site 1 with 67.0% of the total settlement being agents released from Site  
369 1 (Fig. 5). Similarly, total settlement of 75.0, 63.0, and 80.0% at the downstream Sites 2-4  
370 respectively, resulted from agents released from Site 1 thus indicating downstream movement of  
371 agents (Fig. 5). Once again, agents were released from Sites 1 and 3 in the August simulation  
372 (Table 4). The percentage of agent settlement in the August simulation were similar to the July  
373 simulation except settlement at Site 4 consisted entirely of agents released from Site 1 (Fig. 5). In  
374 contrast to the other simulations, agents were released from Sites 1, 2, and 3 in the September  
375 simulation (Table 4). Settlement at Site 1 consisted entirely of self-recruited agents while  
376 settlement from Site 1 agents progressively diminished moving downstream, as agents released  
377 from Site 2 made up 14.0, 9.0, and 38.0% of total site settlement at Sites 2-4, respectively.  
378 However, settlement at the downstream sites was still dominated (50-64%) by the downstream  
379 movement of agents released from Site 1 (Fig. 5).

### 380 **Agent surplus**

381 The present study termed “agent surplus” as non-settled agents present at the completion  
382 of each simulation. Percentage of agent surplus was calculated in each region (identified by colored  
383 regions in Fig. 6) by dividing the number of agents in each region by the total number of agents



384 remaining in the simulation. Overall, the percentage of agent surplus displayed similar trends  
385 between the three simulations, with the greatest variability existing in the Charlotte Harbor and  
386 Gulf of Mexico regions. In each simulation, 56.9-65.7% of the agent surplus existed within the  
387 Gulf of Mexico (Fig. 6 dark blue) as agents were transported out of the system through various  
388 inlets. Pine Island Sound (Fig. 6 blue) and Matlacha Pass (Fig. 6 red) contained 13.0-15.4 and 8.9-  
389 10.9% of the total surplus, respectively (Fig. 6). Surplus in the CRE (Fig. 6 black) was consistently  
390 less than 2.5% (Fig. 6). Charlotte Harbor (Fig. 6 yellow) received 7.7 and 8.9% of the surplus in  
391 the August and September simulations, respectively, with 18.8% surplus in July (Fig. 6).

## 392 **Discussion**

393 The study's promising results serve as a proof of concept that this ABM model can be used  
394 as a viable tool for simulating oyster transport and dispersal dynamics, considering salinity stress  
395 and behavioral aspects of the agents (oyster larvae). Agent survival and settlement data shows that  
396 greater settlement percentage resulted with greater agent survival, which was to be expected as a  
397 larger number of surviving agents would increase the chances of settlement. An in-depth analysis  
398 of the influence of inflow, salinity, and resulting agent survival and settlement is beyond the scope  
399 of this study. However, it is interesting to note that the lowest percentage of agent survival and  
400 settlement occurred in July which also had the lowest minimum, maximum, and mean inflow as  
401 compared to the other simulation months; while the August simulation with the greatest agent  
402 survival and settlement percentages had the greatest mean inflow (Table 5). It was expected that  
403 the simulation month with the greatest inflow (causing reduced salinity) would have resulted in  
404 the lowest agent survival and subsequent settlement. However, these interesting and unexpected  
405 results warrant further investigation in a subsequent study.

406 Overall, the ABM presented in this study reproduced measured larval settlement at the four  
407 monitored sites within the estuarine system. The model recreated the measured settlement pattern  
408 of increasing settlement from Sites 1-3 followed by a reduction in settlement at Site 4 (Figs. 3 - 4).  
409 Additionally, although the model generally (apart from Site 4) overpredicted settlement (at most  
410 by 21.5%) at the individual sites, there was still reasonable agreement between the measured and  
411 simulated settlement (Figs. 3 - 4). However, discrepancies did exist between the measured and  
412 simulated settlement which could be attributed to inaccuracies introduced into the simulations by  
413 the chosen MIKE ECO Lab template parameters (Tables 1-2).

414 For example, the number of agents remaining at the completion of the simulations  
415 (calculated as percentage agent survival; Table 5) provides insight into the combined effects of  
416 natural and salinity-induced mortality. Natural mortality was incorporated into the simulations  
417 through the age-dependent decreasing Weibull function mimicking a Type III survivorship curve  
418 (Table 1; Pinder et al. 1978). Nonetheless, the natural mortality parameters, based on *C. gigas*  
419 oyster larvae, may be over or under-estimating natural mortality found in Gulf of Mexico *C.*  
420 *virginica* larvae. The variability in agent survival can also be attributed to salinity-related mortality  
421 based on salinity tolerance ranges of *C. virginica* oyster larvae from Chesapeake Bay and Long  
422 Island Sound because no tolerance studies were available for the Gulf of Mexico. The template  
423 could be improved through laboratory experiments to determine the specific CHES's larval salinity  
424 tolerances ranges in addition to more accurate information regarding natural mortality within the  
425 system. Furthermore, although the investigation of the influence of inflow, salinity, and resulting  
426 agent mortality is beyond the scope of this study; brief simulation analyses did not indicate a  
427 specific time period(s) within the simulations resulting in an abundance of instantaneous agent

428 mortality. Rather the agents gradually suffered salinity-induced mortality and were removed from  
429 the simulation by low salinities associated with inflow.

430 Despite the differences between measured and simulated settlement, the reasonable  
431 comparison results provided the opportunity to determine connectivity patterns between the four  
432 sites. The simulated results provide strong supporting evidence to Volety et al. (2015) findings of  
433 Site 1's (Fig. 1) role as an important larval source to the downstream Sites (2-4) as well as the  
434 contributions Sites 2 and 3 provide to each other. In summary, agents released from Site 1 provided  
435 at least 50.0% of total settlement at the downstream sites. Additionally, even when agents were  
436 released from three sites as opposed to two, agents released from Site 1 still provided at least 50.0%  
437 of the total settlement at the downstream sites. Site 1's furthest upstream location and importance  
438 as a larval source to the downstream sites could be cause for concern as its upstream location is  
439 likely more impacted by sustained inflow as compared to the other sites (Buzzelli et al. 2013 -  
440 Table 1).

441 Investigation of each simulation revealed four key agent transport patterns (Fig. 6). (1) A  
442 cluster of agents is always transported in the southerly direction out of San Carlos Bay into the  
443 Gulf of Mexico, where the agents generally remain congregated outside of the bay and do not  
444 return into the system. (2) A portion of agents are transported from the CRE into Matlacha Pass  
445 and Pine Island Sound and remain or are further transported into northern Charlotte Harbor. (3)  
446 Agents are transported from the CRE through Matlacha Pass and Pine Island Sound into northern  
447 Charlotte Harbor, and then move through Boca Grande Pass out into the Gulf of Mexico. (4) Few  
448 agents, compared to the total amount released, remain in the CRE near the settlement sites ~12-20  
449 days post release. At the completion of the simulations 56.9-65.7% of surviving, unsettled agents  
450 were transported into the Gulf of Mexico and therefore can be considered lost to the system as

451 those agents generally did not move back into the system (Fig. 6). However, the remaining 34.3-  
452 43.1% of unsettled agents remain within the system’s various regions (Fig. 6) and represent an  
453 “agent surplus”. This surplus has important oyster management and restoration implications by  
454 providing evidence that (1) a large portion of unsettled agents are retained within the system and  
455 (2) a greater abundance of settlement may have occurred if additional settlement sites were  
456 available; future work should include the mapping and monitoring of additional oyster reefs (i.e.  
457 simulation settlement sites), or identification of suitable areas for the creation or enhancement of  
458 reefs. For example, greater measured settlement occurred at Site 4 (Figs. 3 - 4) possibly resulting  
459 from Site 4’s location in Tarpon Bay, a semi-enclosed bay and extension of San Carlos Bay, and  
460 because no agents were released from Site 4 during any simulation (i.e. no measured spawning at  
461 Site 4). However, additional oyster reefs exist within the bay which may have been spawning  
462 during the simulation period, therefore providing larvae to the neighboring sites not captured in  
463 the simulations. Expanding on the most recent oyster reef mapping efforts  
464 ([https://geodata.myfwc.com/datasets/oyster-beds-in-florida?geometry=-82.094%2C26.504%2C-](https://geodata.myfwc.com/datasets/oyster-beds-in-florida?geometry=-82.094%2C26.504%2C-82.012%2C26.518)  
465 [82.012%2C26.518](https://geodata.myfwc.com/datasets/oyster-beds-in-florida?geometry=-82.094%2C26.504%2C-82.012%2C26.518)) and monitoring additional oyster reefs within the CRE will hopefully close  
466 this knowledge gap and improve simulation results.

467 The ABM results provided dispersal patterns between field measured oyster reef sites thus  
468 supporting evidence to previous field based studies (Volety et al. 2015), insight into agent transport  
469 pathways, and resulting “agent surplus”. Insights into transport pathways and “agent surplus” can  
470 aid in selecting locations to construct new oyster reefs as well as deciding which degraded oyster  
471 reefs show the greatest potential for successful restoration (Kim et al. 2013; Smythe et al. 2016;  
472 Arnold et al. 2017). This system-wide approach highlights the oyster reef connectivity and the  
473 relative value of specific reefs and restoration sites in relation to larval supply.

474 Oyster reef restoration efforts since 2016 have occurred throughout San Carlos Bay and  
475 Tarpon Bay with projects adding 10 cm washed fossil shell at elevations from -0.25 m to -0.75 m  
476 National Geodetic Vertical Datum (NGVD). All of the sites (Fig. 7, RS1-RS9) have exhibited  
477 recruitment and have exceeded the targeted live oyster densities greater than 100/m<sup>2</sup> (Fig. 8)(Please  
478 see Text S1 for more detailed description of oyster density calculation). The restoration projects  
479 were planned using habitat suitability models for adult oysters and did not consider the supply and  
480 transport of larvae between existing and restored reefs. The results from this study will be applied  
481 to future restoration planning that seeks a system-wide approach considering larval dispersal  
482 dynamics to improve site selection for future restoration efforts.

483 This ABM framework and study approach is an important tool for the restoration and  
484 management of oyster reefs and can be implemented in other estuaries. Hydrodynamic modeling  
485 of estuaries has greatly increased in the past decades (Brush & Harris 2010), therefore modeling  
486 outputs needed to force the ABM are likely available for most estuaries. The MIKE ECO Lab  
487 template can also be customized to an organism's estuary specific biological characteristics (e.g.  
488 salinity tolerances of Chesapeake Bay oyster larvae). Ultimately, in situ field measurements (e.g.  
489 spawning periods, settlement) may be the limiting factor(s) to attempt a similar study, however  
490 alternative methods are possible. Water temperature measurements are generally available in most  
491 estuaries and can serve as a proxy for histological analysis to initiate spawning events in the  
492 simulations (i.e. agent release)(North et al. 2008; Kim et al. 2010). For example, Volety et al.  
493 (2015) found a range of annual spawning periods in the CRE lasting between 2-9 months  
494 depending on the oyster reef location and inflow, however active spawning closely followed  
495 seasonal water temperature periods greater than 21 °C. Additionally, larval settlement collection  
496 and analysis may be too laborious. An alternative would be to collect bivalve larval concentrations

497 at specific suitable settlement locations (i.e. oyster reefs) and compare field to simulated data with  
498 the assumption that upon reaching a suitable settlement location (i.e. oyster reef), the bivalve  
499 (agent) is classified as settled (Elsäßer et al. 2013). Alternatively, this modeling framework could  
500 first determine locations to implement a field monitoring program, subsequently using the field  
501 measurements to validate the simulated larval transport and dispersal.

502 The utility of using field measurements to validate ABMs and subsequently using ABM  
503 simulation results to pursue future field studies and restoration efforts (or vice versa), is an iterative  
504 process allowing managers and modelers to improve their restoration and research efforts  
505 continuously and collaboratively (Buzzelli et al. 2013). There are inherent positives and negatives  
506 associated with field and modeling studies, as some questions cannot be answered through field or  
507 modeling work alone. However, when used together, field and modeling studies can bolster one  
508 method's finding while introducing new findings and questions that may not have been previously  
509 considered or possible to identify (Ahn et al. 2020; Skogen et al. 2021).

## 510 **Acknowledgments**

511 The authors acknowledge Dr. Aswani Volety and Florida Gulf Coast University Coastal (FGCU)  
512 Watershed Institute for providing the oyster field data. Additional appreciation and gratitude to  
513 DHI for supporting our research through the use of their MIKE software as well as scientist Mikkel  
514 Anderson for his countless support in the development and implementation of the hydrodynamic  
515 model. This work was funded by FGCU Whitaker Center Blair Summer Research Scholarship and  
516 FGCU Graduate Studies Fellowship. Four anonymous reviewers provided numerous comments  
517 that helped to improve the manuscript.

## 518 519 **Literature Cited**

520 Ahn JE, Ronan AD (2020) Development of a model to assess coastal ecosystem health using  
521 oysters as the indicator species. *Estuarine, Coastal and Shelf Science*, 233, 106528

522 Arnold WS, Meyers SD, Geiger SP, Luther ME, Narváez D, Frischer ME, Hofmann E (2017)  
523 Applying a coupled biophysical model to predict larval dispersal and source/sink  
524 relationships in a depleted metapopulation of the eastern oyster *Crassostrea*  
525 *virginica*. *Journal of Shellfish Research*, 36(1), 101-118

526 Baggett LP, Powers SP, Brumbaugh RD, Coen LD, DeAngelis BM, Greene JK, Bushek D (2015)  
527 Guidelines for evaluating performance of oyster habitat restoration. *Restoration*  
528 *Ecology*, 23(6), 737-745

529 Barnes T (2005) Caloosahatchee Estuary conceptual ecological model. *Wetlands*, 25(4), 884–897

530 Barnes TK, Volety AK, Chartier K, Mazzotti FJ, Pearlstine L (2007) A habitat suitability index  
531 model for the eastern oyster (*Crassostrea virginica*), a tool for restoration of the  
532 Caloosahatchee Estuary, Florida. *Journal of Shellfish Research*, 26(4), 949-959

533 Beck MW, Brumbaugh RD, Airoidi L, Carranza A, Coen LD, Crawford C, Defeo O, Edgar GJ,  
534 Hancock B, Kay MC, Lenihan HS, Luckenbach MW, Toropova CL, Zhang G, Guo X  
535 (2011) Oyster reefs at risk and recommendations for conservation, restoration, and  
536 management. *BioScience*, 61(2), 107–116

537 Brush MJ, Harris LA (2010) Advances in modeling estuarine and coastal ecosystems: approaches,  
538 validation and applications. *Ecological Modelling*, 221(7), 965-1088

539 Buzzelli C, Doering PH, Wan Y, Gorman P, Volety A (2013) Simulation of Potential Oyster  
540 Density with Variable Freshwater Inflow (1965–2000) to the Caloosahatchee River  
541 Estuary, Southwest Florida, USA. *Environmental management*, 52(4), 981-994

542 Canal-Verges P, Potthoff M, Hansen FT, Holmboe N, Rasmussen EK, Flindt MR (2014)  
543 Eelgrass re-establishment in shallow estuaries is affected by drifting macroalgae–  
544 Evaluated by agent-based modeling. *Ecological modelling*, 272, 116-128

545 Cavalcante GH, Vieira F, Mortensen J, Ben-Hamadou R, Range P, Goergen E, Campos E, Riegl  
546 B (2020) Biophysical model of coral population connectivity in the Arabian/Persian Gulf.  
547 Elsevier

548 Chamberlain RH, Doering PH (1998) Freshwater inflow to the Caloosahatchee Estuary and the  
549 resource-based method for evaluation. In: Treat SF (ed) Proceedings of the Charlotte  
550 Harbor Public Conference and Technical Symposium. South Florida Water Management  
551 District, Punta Gorda, p 274

552 Connolly SR, Baird AH (2010) Estimating dispersal potential for marine larvae: dynamic models  
553 applied to scleractinian corals. *Ecology*, 91, 3572–3583

554 Davis HC (1958) Survival and growth of clam and oyster larvae at different salinities. *The*  
555 *Biological Bulletin*, 114(3), 296-307

556 Davis HC, Calabrese A (1964) Combined effects of temperature and salinity on development of  
557 eggs and growth of larvae of *M. mercenaria* and *C. virginica*. *Fishery Bulletin*, 63(3), 643-  
558 655

559 DHI Water and environment (2016) MIKE 21 Flow model – FM, User Manual

560 DHI Water and environment (2017) MIKE ECO LAB, Numerical Lab for Ecological and Agent  
561 Based Modelling, User Guide

562 Dye B, Jose F, Allahdadi MN (2020) Circulation Dynamics and Seasonal Variability for the  
563 Charlotte Harbor Estuary, Southwest Florida Coast. *Journal of Coastal Research*, 36(2),  
564 276-288

565 Elsaßer B, Fariñas-Franco JM, Wilson CD, Kregting L, Roberts D (2013) Identifying optimal sites  
566 for natural recovery and restoration of impacted biogenic habitats in a special area of  
567 conservation using hydrodynamic and habitat suitability modelling. *Journal of Sea*  
568 *Research*, 77, 11–21

569 Flaig EG, Srivastava P, Capece JC (1998) Analysis of water and nutrient budgets for the  
570 Caloosahatchee Watershed - Evaluation of available hydrological data for the  
571 Caloosahatchee Watershed. *Southwest Florida Research and Education Center for SWMC*

572 Fisher WS, Winstead, JT, Oliver LM, Edminston HL, Bailey GO (1996) Physiological variability  
573 of eastern oysters from Apalachicola Bay, Florida. *Journal of Shellfish Research*, 15, 543-  
574 555

575 Geyer WR, Signell RP (1992) A reassessment of the role of tidal dispersion in estuaries and  
576 bays. *Estuaries*, 15(2), 97-108

577 Grimm V, Berger U, Bastiansen F, Eliassen S, Ginot V, Giske J, Huth A (2006) A standard  
578 protocol for describing individual-based and agent-based models. *Ecological*  
579 *modelling*, 198(1-2), 115-126

580 Grimm V, Berger U, DeAngelis DL, Polhill JG, Giske J, Railsback SF (2010) The ODD  
581 protocol: a review and first update. *Ecological modelling*, 221(23), 2760-2768

582 Heinänen S, Chudzinska ME, Mortensen JB, Teo TZE, Utne KR, Sivle LD, Thomsen F (2018)  
583 Integrated modelling of Atlantic mackerel distribution patterns and movements: A  
584 template for dynamic impact assessments. *Ecological Modelling*, 387, 118-133

585 International Mussel Watch (1980) National Academy of Sciences, Washington, DC, 248 pp.

586 Kennedy VS (1996) Biology of larvae and spat, in the eastern oyster: *Crassostrea virginica*. In V.  
587 S. Kennedy, R. I. E. Newell & A. F. Eble, editors. The eastern oyster, *Crassostrea*  
588 *virginica*. Maryland Sea Grant, College Park, Maryland, USA, pp. 371-421

589 Kim CK, Park K, Powers SP (2013) Establishing restoration strategy of eastern oyster via a  
590 coupled biophysical transport model. *Restoration Ecology*, 21(3), 353-362

591 Kim CK, Park K, Powers SP, Graham WM, Bayha KM (2010) Oyster larval transport in coastal  
592 Alabama: Dominance of physical transport over biological behavior in a shallow estuary.  
593 *Journal of Geophysical Research*, 115(C10019)

594 Kinne O, Kinne EM (1962) Rates of development in embryos of a cyprinodont fish exposed to  
595 different temperature–salinity–oxygen combinations. *Canadian Journal of Zoology*, 40(2),  
596 231-253

597 Kuusemäe K, von Thenen M, Lange T, Rasmussen EK, Pothoff M, Sousa AI, Flindt MR (2018)  
598 Agent Based Modelling (ABM) of eelgrass (*Zostera marina*) seedbank dynamics in a  
599 shallow Danish estuary. *Ecological Modelling*, 371, 60-75

600 Narváez DA, Klinck JM, Powell EN, Hofmann EE, Wilkin J, Haidvogel DB (2012) Modeling the  
601 dispersal of eastern oyster (*Crassostrea virginica*) larvae in Delaware Bay. *Journal of*  
602 *Marine Research*, 70(2-3), 381-409

603 North EW, Schlag Z, Hood RR, Li M, Zhong L, Gross T, Kennedy VS (2008) Vertical swimming  
604 behavior influences the dispersal of simulated oyster larvae in a coupled particle-tracking  
605 and hydrodynamic model of Chesapeake Bay. *Marine Ecology Progress Series*, 359, 99-  
606 115.

607 Osman RW, Whitlatch RB, Zajac RN (1989) Effects of resident species on recruitment into a  
608 community: larval settlement versus post-settlement mortality in the oyster *Crassostrea*  
609 *virginica*. *Marine Ecology Progress Series*, 61-73



- 610 Pinder JE, Wiener JG, Smith MH (1978) The Weibull distribution: a new method of summarizing  
611 survivorship data. *Ecology*, 59(1), 175-179
- 612 Pine III WE, Walters CJ, Camp EV, Bouchillon R, Ahrens R, Sturmer L, Berrigan ME (2015) The  
613 curious case of eastern oyster *Crassostrea virginica* stock status in Apalachicola Bay,  
614 Florida. *Ecology and Society*, 20(3), 46.
- 615 Pineda J, Hare JA, Sponaugle S (2007) Larval transport and dispersal in the coastal ocean and  
616 consequences for population connectivity. *Oceanography*, 20(3), 22–39
- 617 Rothschild B, Ault J, Gouletquer P, Héral M (1994) Decline of the Chesapeake Bay oyster  
618 population: a century of habitat destruction and overfishing. *Marine Ecology Progress  
619 Series*, 111, 29–39.
- 620 Scarlatos PD (1988) Caloosahatchee estuary dynamics. *Technical Publication 88-7*, Water  
621 Resource Division, Resource Planning Department, South Florida Water Management  
622 District, West Palm Beach, 39p
- 623 Skogen MD, Ji R, Akimova A, Daewel U, Hansen C, Hjøllø SS, van Leeuwen SM, Maar M,  
624 Macias D, Mousing EA, Almroth-Rosell E, Sailley SF, Spence MA, Troost TA, van de  
625 Wolfshaar K (2021) Disclosing the truth: are models better than observations? *Marine  
626 Ecology Progress Series*, in press.
- 627 Smyth D, Kregting L, Elsässer B, Kennedy R, Roberts D (2016) Using particle dispersal models to  
628 assist in the conservation and recovery of the overexploited native oyster (*Ostrea edulis*) in  
629 an enclosed sea lough. *Journal of Sea Research*, 108, 50-59
- 630 Suara K, Chanson H, Borgas M, Brown RJ (2017) Relative dispersion of clustered drifters in a  
631 small micro-tidal estuary. *Estuarine, Coastal and Shelf Science*, 194, 1-15.
- 632 Sun D, Wan Y, Qiu C (2016) Three dimensional model evaluation of physical alterations of the  
633 Caloosahatchee River and Estuary: Impact on salt transport. *Estuarine, Coastal and Shelf  
634 Science*, 173, 16–25
- 635 Tay Y, Todd P, Rosshaug P, Chou L (2012) Simulating the transport of broadcast coral larvae  
636 among the Southern Islands of Singapore. *Aquatic Biology*, 15(3), 283–297
- 637 Volety AK, McFarland K, Darrow E, Rumbold D, Tolley SG, Loh AN (2015) Oyster monitoring  
638 network for the Caloosahatchee Estuary. Final Report, South Florida Water Management  
639 District, West Palm Beach, Florida
- 640 Volety AK, Savarese M, Tolley SG, Arnold WS, Sime P, Goodman P, Doering PH (2009) Eastern  
641 oysters (*Crassostrea virginica*) as an indicator for restoration of Everglades Ecosystems.  
642 *Ecological Indicators*, 9(6), S120–S136
- 643 Wallace RK, Waters P, Rikard FS (2008) Oyster hatchery techniques. Southern Regional  
644 Aquaculture Center.

645  
646 **Illustrations**

647 **Tables**

648 Table 1. Mathematical formulations of the oyster larval agent-based model including functions,  
649 parameters, constants, and forcing. VTS refers to varying in time and space.

650

651

<i>Function / Parameter / Constant</i>	<i>Value</i>	<i>Unit</i>	<i>Equation / References</i>
Age-dependent decreasing Weibull function mimicking Type III survivorship curve	-	-	$f(x) = \frac{\gamma}{\alpha} \left(\frac{x-\mu}{\alpha}\right)^{\gamma-1} \exp\left(-\left(\frac{x-\mu}{\alpha}\right)^\gamma\right)$ Pinder et al. 1978
Shape parameter of the survivorship curve ( $\gamma$ )	0.75	-	Rumrill 1990; Crockett et al. 2012; user defined
Scale parameter of the survivorship curve ( $\alpha$ )	0.1	-	Rumrill 1990; Crockett et al. 2012; user defined
Minimum daily instantaneous mortality rate	0.01	day <sup>-1</sup>	Rumrill 1990; user defined
Maximum daily instantaneous mortality rate	0.12	day <sup>-1</sup>	Rumrill 1990; user defined
Development period before agent becomes competent to settle	10	days	$T_{\text{larvae}} = 110.79 \times \exp(-0.0825 \times T_w)$ $T_w = \text{water temperature } ^\circ\text{C}$ $T_{\text{larvae}} = \text{larval period (in days)}$ Kennedy 1996; Table S1 - water temperature $^\circ\text{C}$
Settling speed - development period	0	m/s	Kim et al. 2010
Settling speed - post development period	0.007	m/s	Hidu & Haskin 1978; Kim et al. 2010
Maximum planktonic larval (agent) duration	25	days	Kennedy 1996; Narvaez et al. 2012
Maximum distance from agent to suitable settlement substrate (site) for settlement	0.5	m	Cavalcante et al. 2020
Minimum water depth at which at agent can settle	0.01	m	Volety et al. 2003; user defined
Maximum water depth at which at agent can settle	4.0	m	Volety et al. 2003; user defined
Maximum current speed for agent settlement	1.0	m/s	Cavalcante et al. 2020; user defined
<i>Forcing</i>	<i>Value</i>	<i>Unit</i>	<i>References</i>
Horizontal current direction (HD)	VTS	Degrees	Data extracted from Dye et al., 2020 HD
Horizontal current speed (HD)	VTS	ms <sup>-1</sup>	Data extracted from Dye et al. 2020 HD
Vertical current speed (HD)	VTS	ms <sup>-1</sup>	Data extracted from Dye et al. 2020 HD
Water Elevation (HD)	VTS	m	Data extracted from Dye et al. 2020 HD
Horizontal dispersion	1.0	scaled eddy viscosity formulation	DHI, 2016; Cavalcante et al. 2020; user defined
Salinity	VTS	PSU	See Table S1.

653

654

655

656

657 Table 2. Mathematical formulations of the Eastern oyster (*C. virginica*) larval agent-based model

658 salinity tolerance ranges.

<i>Salinity tolerance range (PSU)</i>	<i>Equation</i>	<i>Maximum time before mortality (days)</i>	<i>References</i>	<i>Salinity rejuvenation timer (days)</i>	<i>References</i>
7.5-10	IF SALDUR1/24 > saldur_thres1 THEN REMOVE { (OYS, 1)} ELSE 0	7	Davis 1958; David & Calabrese 1964	1	Kinne & Kinne 1962; user defined
5.0-7.5	IF SALDUR2/24 > saldur_thres2 THEN REMOVE { (OYS, 1)} ELSE 0	2	Davis 1958; David & Calabrese 1964	1	Kinne & Kinne 1962; user defined
<5.0	IF SALDUR3/24 > saldur_thres3 THEN REMOVE { (OYS, 1)} ELSE 0	0.25	Davis 1958; David & Calabrese 1964	1	Kinne & Kinne 1962; user defined

SALDUR(1,2,3) refers to Maximum time before mortality (days)

saldur\_thres(1,2,3) refers to Salinity tolerance range (PSU)

OYS refers to "Particle Classes" in ECOLab template

659

660

661 Table 3. Model sensitivity testing performed with the August 2011 simulation comparing the

662 relative percentage of total and individual site settlement.

<i>Site</i>	<i>2,500 agents</i>	<i>Settlement (%)</i>	<i>5,000 agents</i>	<i>Settlement (%)</i>	<i>10,000 agents</i>	<i>Settlement (%)</i>
1	6	0.24	4	0.08	17	0.17
2	72	2.88	121	2.42	236	2.36
3	99	3.96	178	3.56	313	3.13
4	4	0.16	7	0.14	16	0.16
Total	181	7.24	310	6.20	582	5.82

663

664

665 Table 4. Model simulation periods, locations, and number of agents released.

666

<i>Year</i>	<i>Simulation period</i>	<i>Agent sources</i>	<i>Total amount of agents released</i>
	July 5-30th	Sites 1 and 3	5000
2011	August 5-30th	Sites 1 and 3	5000
	September 5-30th	Sites 1, 2, and 3	7500

667

668

669

670

671

672 Table 5. Percent agent survival (agents in the water column + settled) and agent settlement at the  
 673 end of each simulation period and freshwater inflow at S-79 during the simulation period.

<i>Year</i>	<i>Simulation period</i>	<i>Agent survival (%)</i>	<i>Agent settlement (%)</i>	<i>Inflow min – max; mean ± SD (m<sup>3</sup>/s)</i>
	July 1-30	13.4	1.2	5.7 - 59.5; 30.9 ± 14.1
2011	August 1-30	15.8	3.6	12.7 - 84.6; 48.4 ± 18.3
	September 1-30	14.8	2.0	12.7 - 135.1; 45.6 ± 30.2

674  
 675 **Figure captions**

676 **Figure 1.** Map of the Charlotte Harbor estuarine system (CHES) study area showing the  
 677 Caloosahatchee River Estuary (CRE) (cross hatch region), oyster reef monitoring sites and agent  
 678 release locations (1-4), and water quality monitoring stations (A-J).

679  
 680 **Figure 2.** The hydrodynamic model (HD) computational mesh (A), zoomed-in view of the  
 681 Caloosahatchee River Estuary (CRE) (B), and two-dimensional depth-averaged salinity grid (C).

682  
 683 **Figure 3.** Percentage of monthly settlement measured (gray bars) and simulated (black bars) at  
 684 Sites 1 to 4. Calculated by (specific monthly settlement (simulated or measured) at a specific  
 685 site/total specific monthly settlement (simulated or measured) at all sites) x100.

686  
 687 **Figure 4.** Percentage of total settlement measured (gray bars) and simulated (black bars) at Sites  
 688 1 to 4. Calculated by (total settlement from each (simulation or measurement) at a specific site/total  
 689 settlement from each (simulation or measurement) at all sites) x100.

690  
 691 **Figure 5.** Connectivity between the four oyster reefs (numbers 1 to 4 in the top left map)  
 692 established from July, August, and September 2011 simulations. The different colored sectors

693 represent the percentage of agents settled at each site respectively released at Sites 1 (blue), 2  
694 (yellow), and 3 (gray).

695

696 **Figure 6.** Distribution of agents (white circles) and percentage of agent surplus in each region  
697 (demarcated by colored areas) at the conclusion of each 2011 monthly simulation.

698

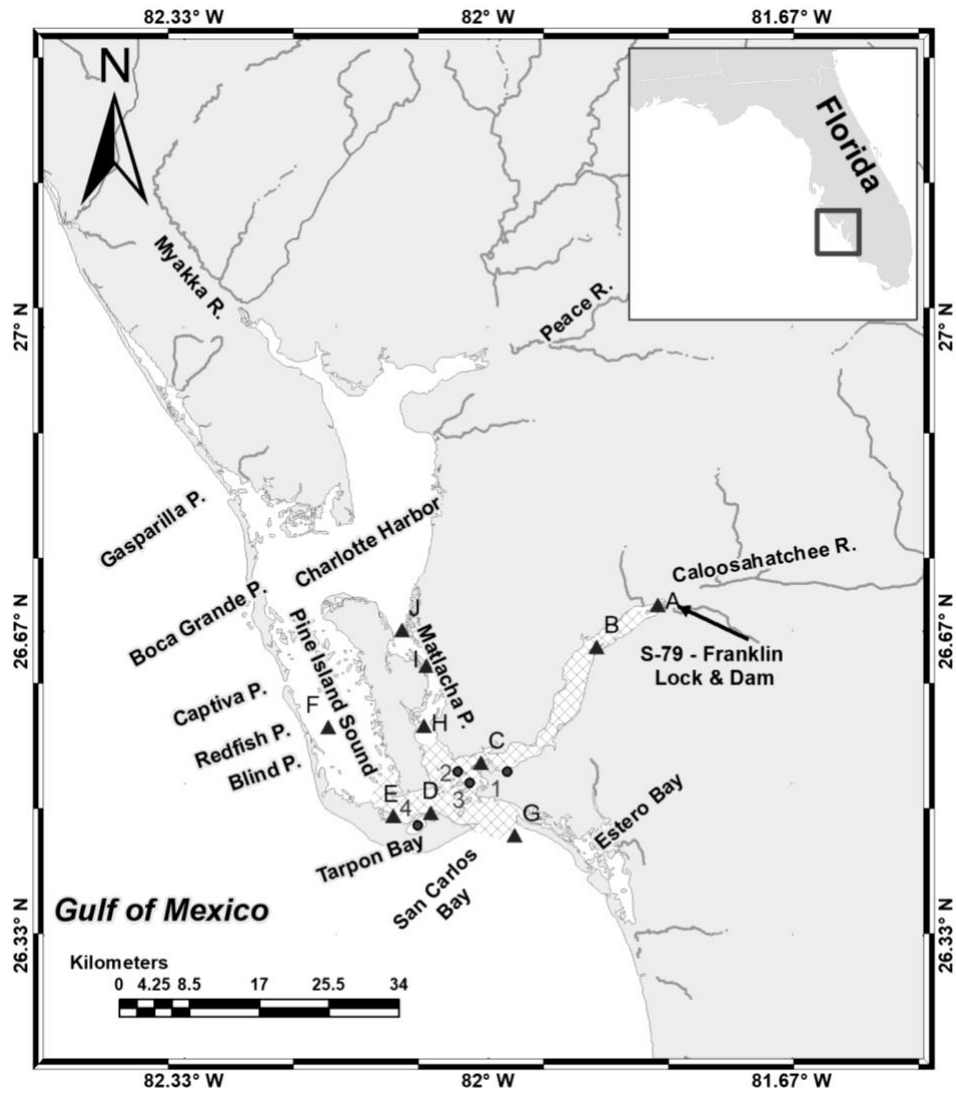
699 **Figure 7.** Oyster reef sites 2016-2020: reference (RS1,4,7), restored (RS2,5,8), and control  
700 (RS3,6,9).

701

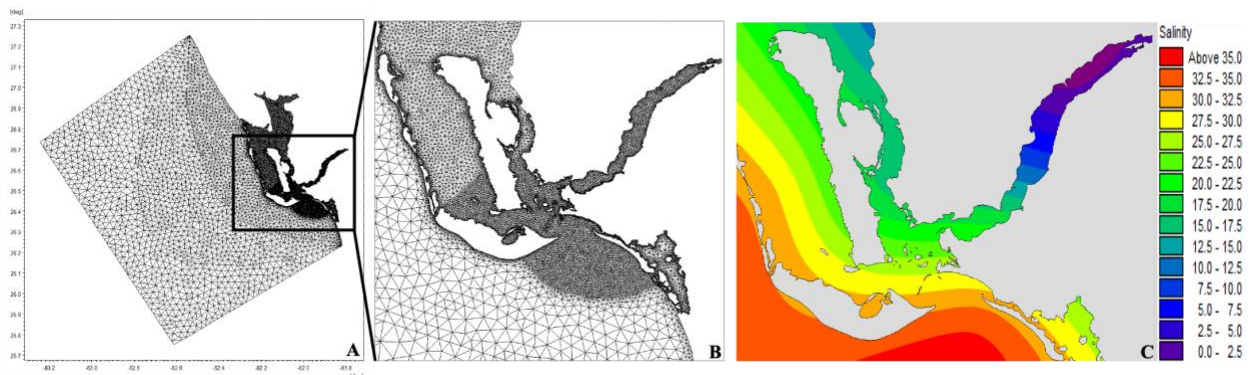
702 **Figure 8.** Eastern oyster (*Crassostrea virginica*) density and error bars indicating the standard  
703 error at restored, reference, and control sites. Please note the different y axis values. (A) upper San  
704 Carlos Bay, (B) lower San Carlos Bay, (C) Tarpon Bay. Fossil shell substrate was added to  
705 Restored Reefs at time = 0. Pre-construction monitoring at all sites occurred 1 year prior to  
706 construction (year = -1). Reference reefs are near restored reefs and are thought to represent healthy  
707 reefs. Control sites were at similar elevations to reference and restored reefs but had few live  
708 oysters.

709

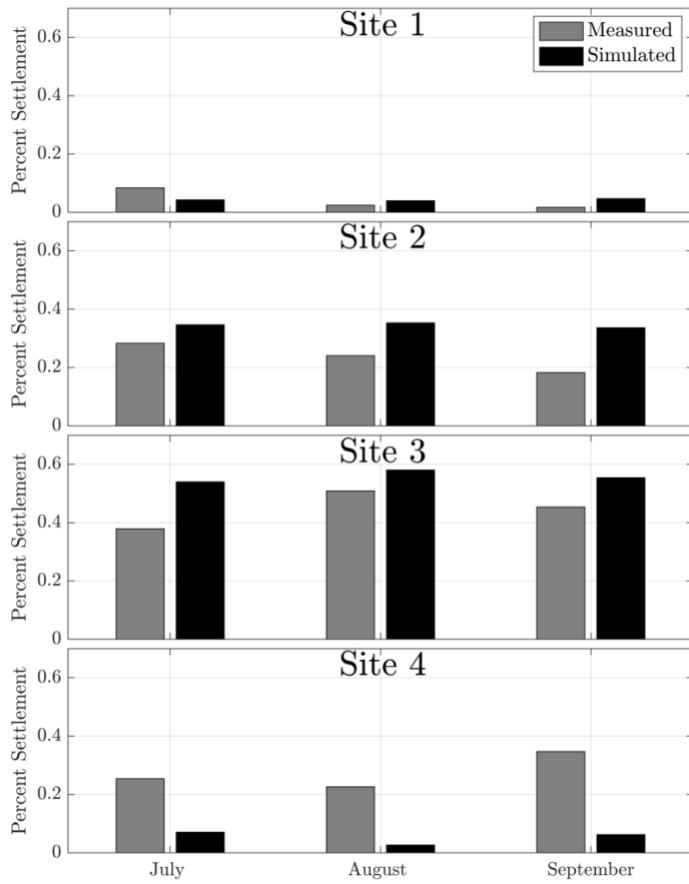
710 **Figures**



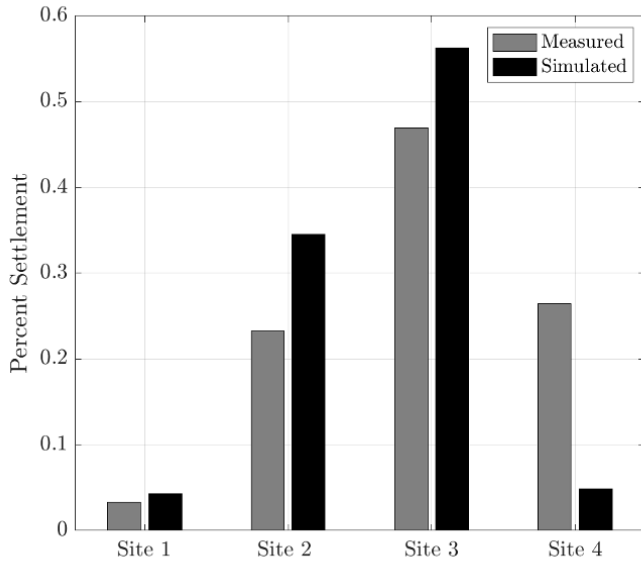
711  
712  
713



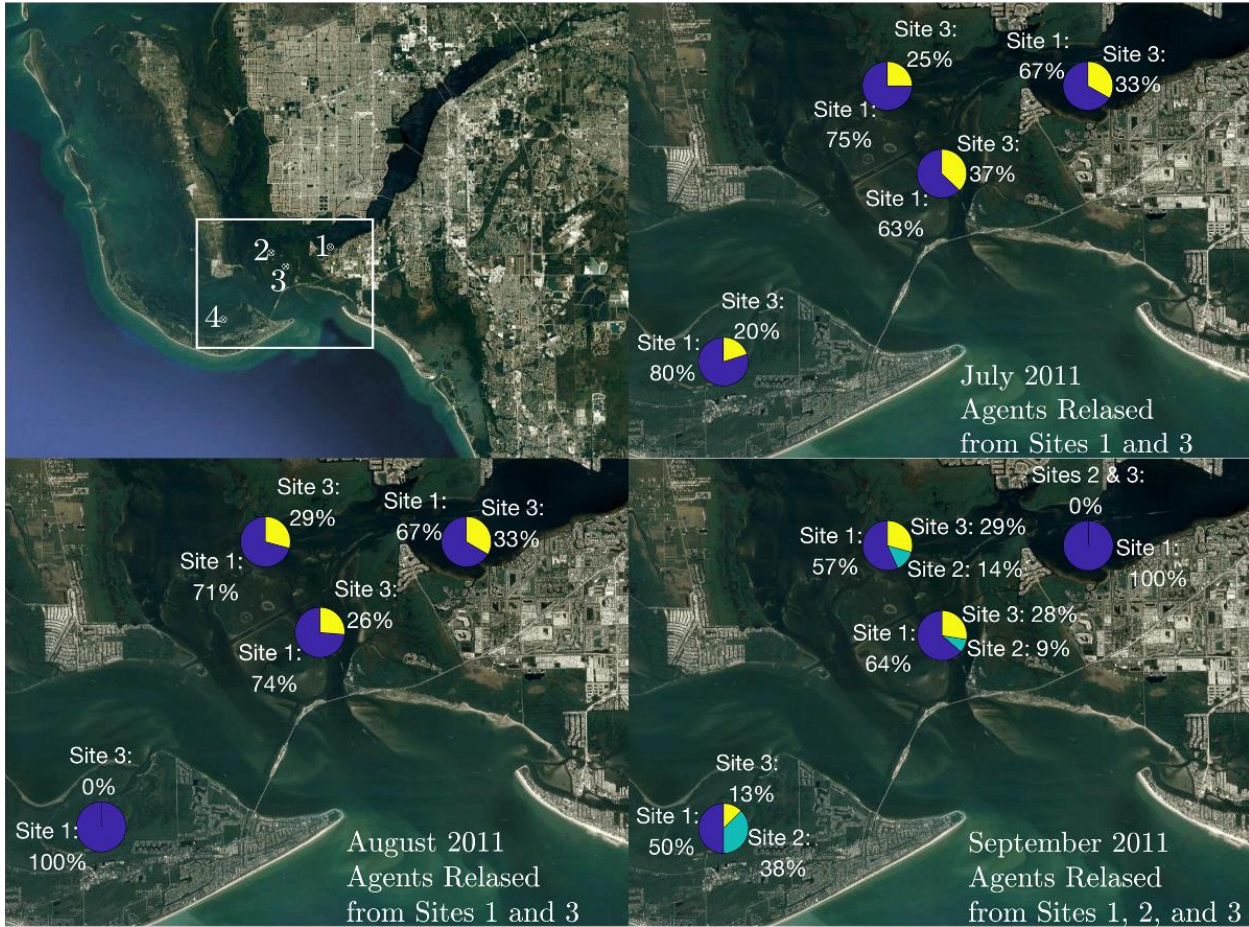
714  
715  
716  
717



718

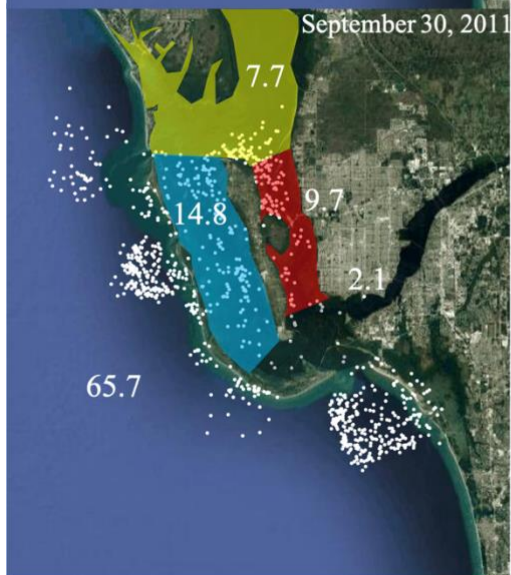
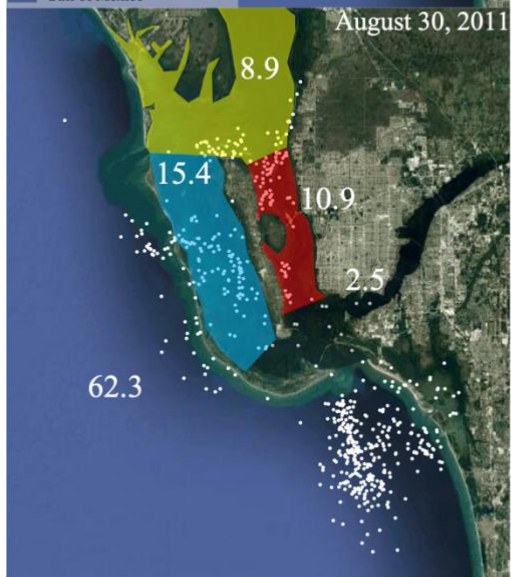
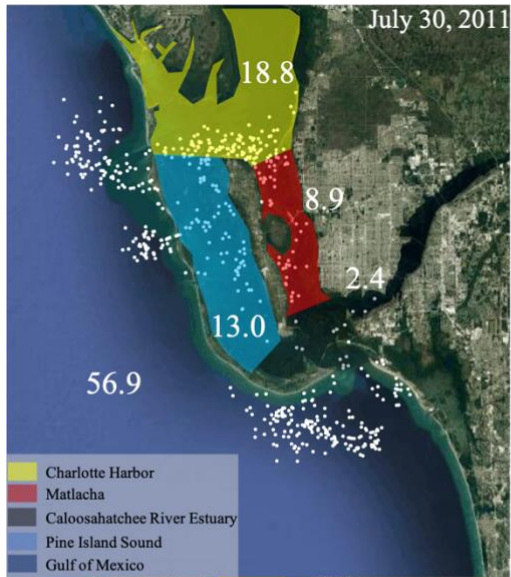


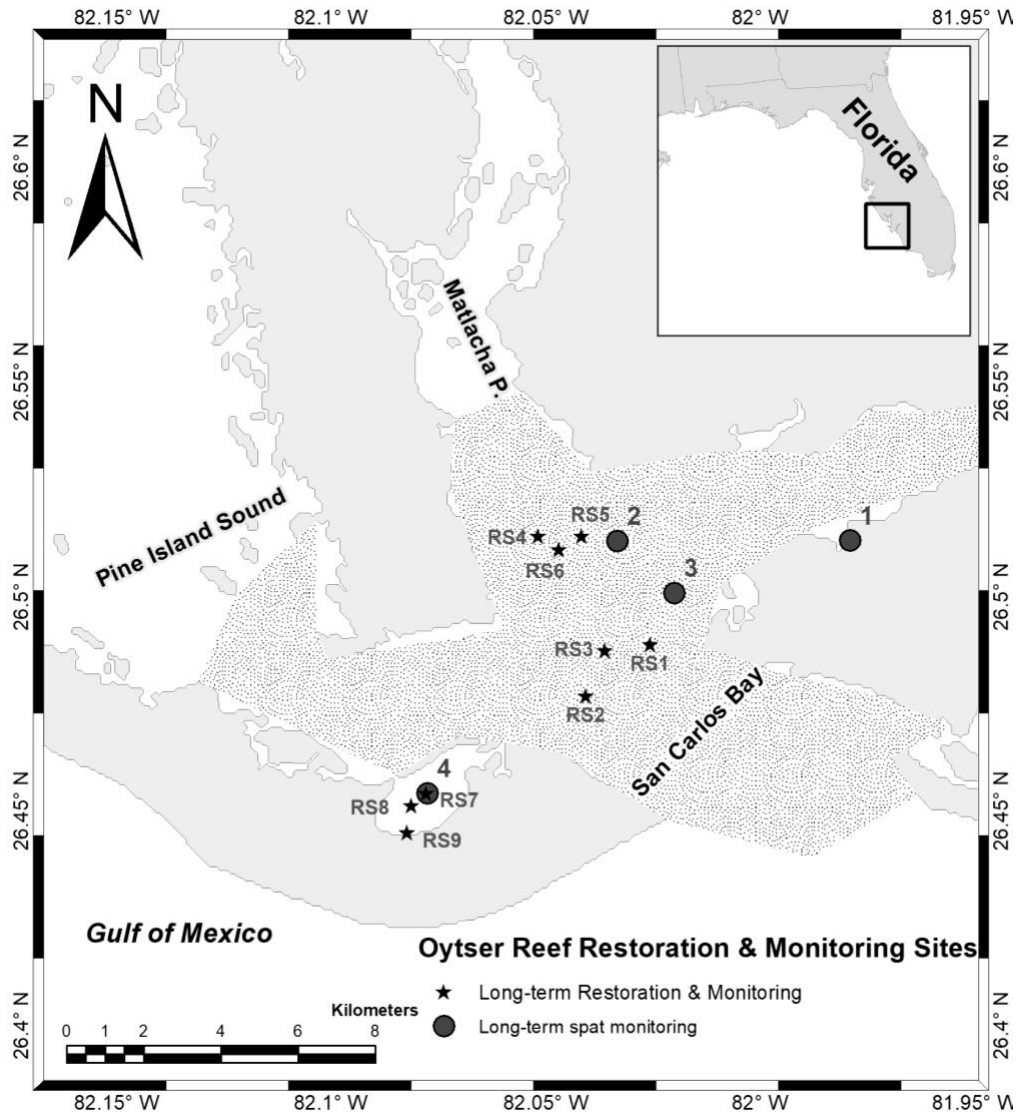
719  
720

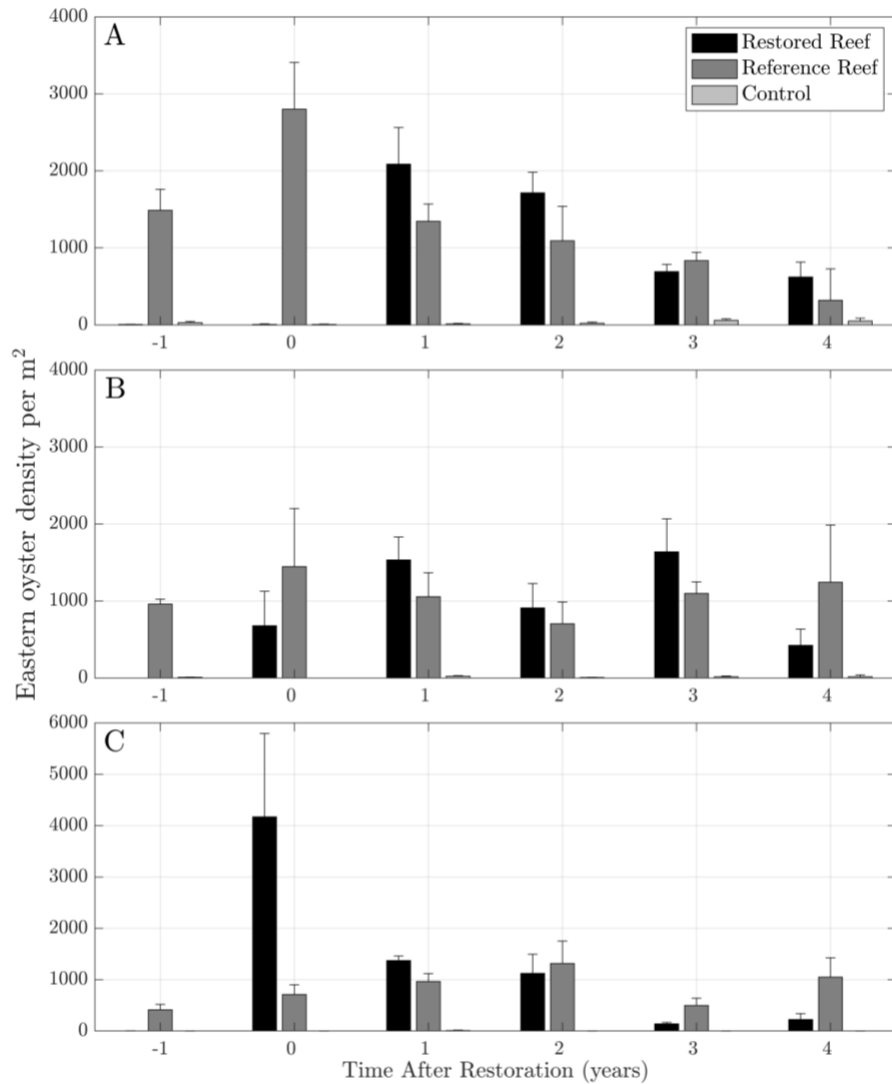


721  
722









725  
726  
727  
728

### Supporting Information

729 Text S1. In a separate oyster monitoring study (2015-2020), oyster densities were collected during  
730 pre- and post-restoration at restored, reference, and control sites following Baggett et al. (2016).  
731 The footprint and elevation of each site were determined using a Trimble RTK GPS. A grid of  
732 points was overlaid on the footprint to determine quadrat placement. The points were assigned a  
733 random number and then each quadrat was collected using a handheld Garmin GPS to locate the  
734 point. Five quadrats were placed and all shell and material within the quadrats were collected in a  
735 bucket and returned to the lab for enumeration and measurement. Quadrat size was determined

736 using a power analysis. A 1 m<sup>2</sup> quadrat was used for the control sites and pre-restoration sampling  
 737 and 0.25 m<sup>2</sup> was used for reference and post-restoration sampling. Sampling started in March 2015  
 738 and occurred annually through 2020.

739  
 740 Table S1. Continuous environmental data series available within the Charlotte Harbor estuarine  
 741 system: data source, stations names, and parameters measured (RECON hourly, CHAP 15  
 742 minute) at the different stations. SCCF: Sanibel-Captiva Conservation Foundation; CHAP:  
 743 Charlotte Harbor Aquatic Preserve.

<i>Data source</i>	<i>Station name by the source</i>	<i>Station letter on Figure 1.</i>	<i>GPS position</i>	<i>Parameters measured and years of collection</i>
SCCF - RECON	Beautiful Island	A	26.695, -81.814	Salinity (PSU) Water temperature (°C) 2013-Present
	Fort Myers	B	26.649, -81.881	Salinity (PSU) Water temperature (°C) 2008-Present
	Shell Point	C	26.523, -82.008	Salinity (PSU) Water temperature (°C) 2008-Present
	Tarpon Bay	D	26.468, -82.063	Salinity (PSU) Water temperature (°C) 2011-Present
	McIntyre Creek	E	26.465, -82.104	Salinity (PSU) Water temperature (°C) 2014-Present
	Redfish Pass	F	26.562, -82.175	Salinity (PSU) Water temperature (°C) 2008-Present
	Gulf of Mexico	G	26.443, -81.971	Salinity (PSU) Water temperature (°C) 2008-Present
CHAP	MP2B	H	26.563, -82.070	Salinity (PSU) Water temperature (°C) 2005-Present
	MP3C	I	26.629, -82.067	Salinity (PSU) Water temperature (°C) 2009-Present

744  
745  
746

---

	MP1A	J	26.668, -82.095	Salinity (PSU) Water temperature (°C) 2005-Present
--	------	---	-----------------	--